Ecological Modelling 260 (2013) 25–35

Contents lists available at SciVerse ScienceDirect

Ecological Modelling

journal homepage: www.elsevier.com/locate/ecolmodel

Incorporating weather sensitivity in inventory-based estimates of boreal forest productivity: A meta-analysis of process model results

Z. Wang[a], R.F. Grant[a], M.A. Arain[b], P.Y. Bernier[c,*], B. Chen[b], J.M. Chen[d], A. Govind[d], L. Guindon[c], W.A. Kurz[e], C. Peng[f], D.T. Price[g], G. Stinson[e], J. Sun[f], J.A. Trofymowe[e], J. Yeluripati[b]

[a] Department of Renewable Resources, University of Alberta, Edmonton, AL, Canada
[b] School of Geography and Earth Sciences and McMaster Centre for Climate Change, McMaster University, Hamilton, ON, Canada
[c] Canadian Forest Service, Laurentian Forestry Centre, Quebec, QC, Canada
[d] Department of Geography and Program in Planning, University of Toronto, Toronto, ON, Canada
[e] Canadian Forest Service, Pacific Forestry Centre, Victoria, BC, Canada
[f] Institute of Environment Sciences, University of Quebec at Montreal, Montreal, QC, Canada
[g] Canadian Forest Service, Northern Forestry Centre, Edmonton, AL, Canada

ARTICLE INFO

Article history:
Received 28 November 2012
Received in revised form 24 March 2013
Accepted 26 March 2013
Available online 30 April 2013

Keywords:
Ecosystem modeling
Carbon flux
Forest productivity
CBM-CFS3
Ecosys
Can-IBIS
CN-CLASS
InTEC
TRIPLEX

ABSTRACT

Weather effects on forest productivity are not normally represented in inventory-based models for carbon accounting. To represent these effects, a meta-analysis was conducted on modeling results of five process models (*ecosys*, *CN-CLASS*, *Can-IBIS*, *InTEC* and *TRIPLEX*) as applied to a 6275 ha boreal forest landscape in Eastern Canada. Process model results showed that higher air temperature (T_a) caused gains in CO_2 uptake in spring, but losses in summer, both of which were corroborated by CO_2 fluxes measured by eddy covariance (EC). Seasonal changes in simulated CO_2 fluxes and resulting inter-annual variability in NEP corresponded to those derived from EC measurements. Simulated long-term changes in above-ground carbon (AGC) resulting from modeled NEP and disturbance responses were close to those estimated from inventory data. A meta-analysis of model results indicates a robust positive correlation between simulated annual *NPP* and mean maximum daily air temperature (T_{amax}) during May–June in four of the process models. We therefore, derived a function to impart climate sensitivity to inventory-based models of NPP: $NPP'_i = NPP_i + 9.5\,(T_{amax} - 16.5)$ where NPP_i and NPP'_i; are the current and temperature-adjusted NPP, 16.5 is the long-term mean T_{amax} during May–June, and T_{amax} is that for the current year. The sensitivity of net CO_2 exchange to T_a is nonlinear. Although, caution should be exercised while extrapolating this algorithm to regions beyond the conditions studied in this landscape, results of our study are scalable to other regions with a humid continental boreal climate dominated by black spruce. Collectively, such regions comprise one of the largest climatic zones in the 450 Mha North American boreal forest ecosystems.

1. Introduction

Boreal forests account for about 14% of the earth's vegetation cover (Kang et al., 2006) and contain large amounts of carbon (C) (D'Arrigo et al., 1987; Sun et al., 2008). The capability of boreal forests to capture and release C is governed by climate and disturbance (Amiro et al., 2001; Banfield et al., 2002; Rapalee et al., 1998). In Canada, the influence of climate and disturbance on boreal forests has drawn much attention (Chertov et al., 2009; Bergeron et al., 2007), given that about 30% of the world's boreal forests are located in Canada (Canadian Forest Service, 2009). Improved understanding of the responses of boreal forest productivity to climate and disturbance is necessary to project future changes in forest C productivity and storage in a region exposed to rapid changes in climate.

The productivity of the boreal forest, and hence its C dynamics, are influenced by short-term and long-term variability in climate. For example, higher spring air temperatures (T_a) create longer growing seasons which have been found to raise seasonal productivity through earlier net CO_2 uptake (Arain et al., 2002; Barr et al., 2004; Bergeron et al., 2007; Brooks et al., 1998; Delpierre et al., 2009; Grant et al., 2009a,b; Wilmking et al., 2004). On the other hand, higher summer T_a has been found to reduce productivity (Brooks et al., 1998; Dang and Lieffers, 1989; Tang et al., 2010) through concurrent declines in gross primary productivity (GPP) and increased ecosystem respiration (R_e) (Grant et al., 2009b; Griffis et al., 2003; Morgenstern et al., 2004), and through adverse effects on tree water status (Barber et al., 2000; Goetz et al., 2005;

* Corresponding author. Tel.: +1 418 648 4524; fax: +1 418 648 5849.
E-mail addresses: pbernier@rncan.gc.c, pierre.bernier@nrcan.gc.c (P.Y. Bernier).

0304-3800/$ – see front matter.
http://dx.doi.org/10.1016/j.ecolmodel.2013.03.016

Savva et al., 2008). Gains in productivity from higher spring or summer T_a are likely the more important responses in cooler or wetter climates, while losses in productivity resulting from higher summer T_a are likely to be more important in warmer or drier climates (e.g. Hofgaard et al., 1999; Nishimura and Laroque, 2011).

In Canada, the accounting and reporting on the state of, and changes in, forest C are done using the *CBM-CFS3* model (Kurz et al., 2009), which constitutes the core component of Canada's National Forest Carbon Monitoring, Accounting, and Reporting System (NFCMARS, Kurz and Apps, 2006). In this inventory-based model, estimates of forest productivity are generated from forest growth curves and do not explicitly consider variability in climate (Kurz et al., 2009). One question that was raised in the Fluxnet-Canada Research Network/Canadian Carbon Program (FCRN/CCP) (Margolis et al., 2006) was whether and how climatic sensitivity should be incorporated into *CBM-CFS3*. The FCRN/CCP therefore conducted a meta-analysis of results from multiple process models as applied to two contrasting forest landscapes centered on FCRN/CCP flux measurement sites: a coastal temperate forest landscape in British Columbia, and a continental boreal forest landscape near Chibougamau, in Quebec. Results from the coastal temperate forest modeling analysis (Wang et al., 2011) showed a convergence of climate sensitivity among process models for simulating weather effects on CO_2 exchanges. The result of the meta-analysis was a simple temperature-based equation to adjust CBM-CFS3 estimates of productivity to climate. However, the adjustment was considered appropriate only for the Pacific coastal region and not suitable for application in other climatic regions of Canada.

The current study builds on this work, but with a focus on the boreal forest landscape. The objectives of this study were (1) to determine the extent to which seasonal variability in weather affects modeled and measured productivity at seasonal to annual time scales, and (2) to extract a robust relationship between seasonal variability in weather and interannual variability in productivity that could be used to impart climate sensitivity to inventory models of forest productivity. Central to this investigation was an initial evaluation of the capacity of our suite of process-based models to reproduce the CO_2 flux measurements made at the boreal forest site at hourly and daily time scales. All abbreviations in the text below are listed in Table 1. In this analysis, total ecosystem C is defined as the sum of above-ground biomass (living) C (AGC), surface dead C (SDC), and below-ground organic live or dead C (BGC).

Table 1
List of abbreviations.

AGC	Above-ground biomass (living) C
APAR	Absorbed photosynthetically active radiation
BGC	Below-ground C (live roots, dead roots, and soil)
Can-IBIS	Canadian version of the Integrated Biosphere Simulator
CBM-CFS3	Carbon Budget Model of the Canadian Forest Service
CCP	Canadian Carbon Program
CN-CLASS	Carbon–Nitrogen version of the Canadian Land Surface Scheme
D	Vapor pressure deficit
EOBS	Eastern Old Black Spruce FCRN flux tower site at Chibougamau
DIC	Dissolved inorganic C
DOC	Dissolved organic carbon
DOM	Dead organic matter carbon
EC	Eddy covariance
ε_g	Gross photosynthetic efficiency
FCRN	Fluxnet Canada Research Network
GIS	Geographic information system
GPP	Gross primary productivity
g_c	Canopy conductance
g_l	Leaf conductance
InTEC	Integrated Terrestrial Ecosystem C-budget model
J	Electron transport rate
LAI	Leaf area index
LE	Latent heat flux
MAT	Mean annual air temperature
MSC	Meteorological Service of Canada
NPP	Net primary productivity
NEP	Net ecosystem productivity
NBP	Net biome productivity
OR	Oyster River region of Vancouver Island
Ω_a	Root axial resistance
Ω_r	Root radial resistance
PFT	Plant functional type
R_a	Autotrophic respiration
R_e	Ecosystem respiration
R_g	Growth respiration
R_h	Heterotrophic respiration
RMSD	Root mean square for difference
R_m	Maintenance respiration
SDC	Surface dead carbon (standing dead, stumps, forest floor)
SLC	Soil Landscapes of Canada
T_a	Air temperature
T_{amax}	Mean daily maximum air temperature during May – June
T_c	Canopy temperature
T_s	Soil temperature
θ_s	Available water content in soil
V_c	Canopy CO_2 fixation rate
V_r	Rubisco-limited CO_2 fixation rate
ψ_r	Root water potential
ψ_T	Canopy turgor potential
ψ_C	Canopy water potential

2. Model descriptions

The model intercomparison involved one inventory model *CBM-CFS3* (Kurz et al., 2009) and five process models developed in Canada: *ecosys* (Grant et al., 2007), *CN-CLASS* (Arain et al., 2006), *Can-IBIS* (Liu et al., 2005), *InTEC* (Chen et al., 2003) and *TRIPLEX* (Peng et al., 2002). The choice of the process models was based on their demonstrated ability to simulate climate effects on boreal ecosystem productivity (Grant et al., 2005, 2009a,b; Arain et al., 2002, 2006; Liu et al., 2005; Chen et al., 2000; Sun et al., 2008). The inventory model *CBM-CFS3* and the process models *ecosys*, *CN-CLASS*, *Can-IBIS* have also been used in the coastal temperate forest landscape intercomparison exercise and are therefore described in Wang et al. (2011). For the sake of parsimony, we provide below only descriptions of the two new models for this exercise: *InTEC* and *TRIPLEX*. Further details on algorithms used in all process models are provided in the Supplementary Material for this paper.

2.1. Integrated Terrestrial Ecosystem C-budget model (InTEC)

InTEC (Integrated Terrestrial Ecosystem C-budget model) was developed to simulate the integrated effects of disturbances, management practices, climate, and atmospheric factors at regional and global scales (Chen et al., 2000, 2003). The model simulates the dynamics of forest carbon stocks at an annual step through an up-scaling algorithm for the leaf-level model and combines the upscaled results with an age-NPP relationship. Inputs include climate, soil texture, nitrogen deposition, forest stand age and vegetation parameters (e.g. leaf area index and land cover type which can be generated from remotely sensed data).

2.2. TRIPLEX

The *TRIPLEX* model was developed at the Ontario Forest Research Institute of the Ontario Ministry of Natural Resources through collaboration with the Faculty of Natural Resources Management of Lakehead University. The model was developed on the basis of three models, namely *3PG* (Landsberg and Waring, 1997), *TREEDYN* 3.0 (Bossel, 1996) and *CENTURY* 4.0 (Parton et al., 1993) to simulate forest growth and the dynamics of carbon and nitrogen. Modeling processes of *TRIPLEX* have been described in detail by Peng et al. (2002) and Liu et al. (2002).

Calculations were performed on a monthly time step for C flux and allocation, and on an annual time step for tree growth, and the budgets of C, N, and water. Forest growth and C and N dynamics in the model are primarily driven by climatic variables (e.g. T_a and precipitation) and solar radiation. Other inputs include environmental factors (soil water holding capacity and N) and biological factors (forest age, biomass allocation, tree form and mortality).

3. Modeling experiment

3.1. Study area

3.1.1. General features

The Chibougamau boreal forest study area (49°38′44″–49°42′39″ N; 74°23′39″–74°15′31″ W, Fig. 1) covers 6275 ha. It has a continental boreal climate with a mean annual T_a of 0 °C and annual precipitation of 961 mm. Dominant tree species include black spruce (*Picea mariana* (Mill.), jack pine (*Pinus banksiana* Lamb.) and trembling aspen (*Populus tremuloides* Michx.) (Fig. 1).

Five soil types in the Chibougamau study area (fluvio-glacial, fine glacial till, coarse glacial till, deep organic and shallow organic) were identified from a vector map of surficial deposit type and soil texture properties. Soil types in each map polygon were allocated to 100 m × 100 m grid cells based on the soil type at the grid cell's centroid. Key properties for soil horizons (field capacity, wilting point, coarse fraction, pH, organic C, total N, and drainage) were derived from the Soil Landscapes of Canada (SLC Version 3.1) in the CanSIS National Soil Database (CanSIS, 2006). The fluvio-glacial, deep organic and shallow organic soil types were poorly drained (water table depth 0.20 m in spring and 0.80 m in summer). Both fine and coarse glacial tills were well drained.

3.1.2. Forest types and disturbances

A complete description of the procedure for characterizing the evolution of the forest in the Chibougamau study area can be found in Bernier et al. (2010). Briefly, polygon-based forest cover for the Chibougamau study area in 1928 was interpreted from aerial photographs at a scale of 1:12,000, whereas forest cover in 1998 was extracted from a forest cover map at a scale of 1:20,000. These forest covers were used in conjunction with the Provincial merchantable volume database to estimate AGC over the study area in 1928 and 1998 (Bernier et al., 2010). Forest types in each map polygon were allocated to the same 100 m × 100 m grid cells used for soil types based on the forest type at the grid cell's centroid. The 1928 aerial photographs were also used to bin forest stand ages in 1928 into classes of 10, 30, 50, 70, 90 and 120 years for use in model spin-up. To make the forested area consistent among models, only 3825 grid cells that were forested in both 1928 and 1998 were modeled in this study.

Disturbances were identified from aerial photos taken in 1953–1954, 1958–1959, 1965, 1967–1968, 1969–1970, 1982 and 1998, while disturbances more recent than 1970 were identified from forest inventory maps. About 25% of the 3825 ha forested area was disturbed during 1928–2005 by harvesting (either clearcut or partial cut), or insect herbivory. The main disturbance period was in 1963 when 608 ha were clearcut (Fig. 2). These disturbances were allocated to the 100 m × 100 m grid cells used for forest and soil types for the years in which they occurred. Disturbance coefficients used in *CBM-CFS3* to estimate transfers of C among model pools for each disturbance type (Kurz et al., 2009) were adopted in all of the process models.

3.1.3. CO_2 fluxes and weather data

A flux measurement tower was established in 2003 at the Eastern Old Black Spruce (EOBS) site within the Chibougamau study

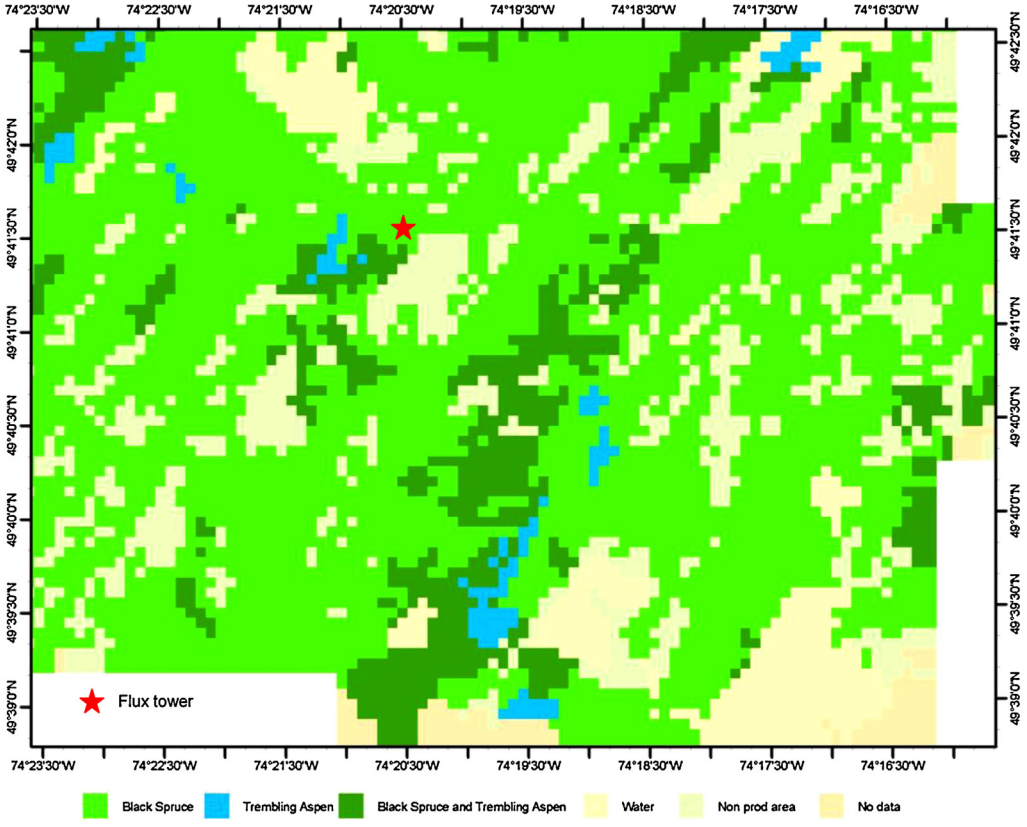

Fig. 1. Location of Chibougamau study area and spatial distribution of tree species groups in 1998. The flux tower is also shown.

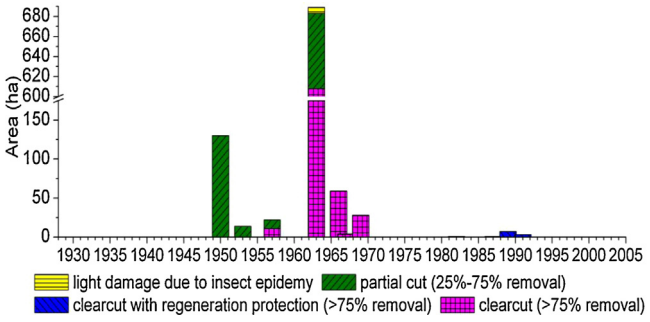

Fig. 2. Area affected by disturbances from 1928 to 2005.

area as part of the Fluxnet Canada Research Network/Canadian Carbon Program (FCRN/CCP) (Bergeron et al., 2007; Coursolle et al., 2006; Fig. 1). Gap-filling of CO_2 fluxes was carried out following Barr et al. (2004). We used the CO_2 flux measurements from 2004–2008 to test models results at daily and monthly time scales by comparing with measured EC fluxes, prior to model application at annual time scales for the study period from 1928–2008.

Daily minimum and maximum T_a and daily precipitation were derived from historical weather records in the Chibougamau region from 1928 to 2003. Daily shortwave radiation during this period was estimated from daily minimum and maximum T_a. Daily wind speeds during this period were taken from those measured at the EOBS flux tower in 2004. However, from 2004 to 2008, half-hourly weather data (radiation, T_a, humidity, wind speed and precipitation) were acquired from the EOBS flux tower (Fig. 1). Thus a continuous weather record was constructed with daily data from 1928 to 2003, followed by half-hourly data from 2004 to 2008. Each model adapted this record to its own time step according to its specific protocols.

3.2. Modeling protocol

The modeling protocol was similar to that described in Wang et al. (2011). Briefly, model runs were performed using the attributes of the soil and plant types and the disturbances derived from maps of the study area, for the 3825 grid cells known to be forested throughout the 1928–1998 period. In *ecosys* and *CN-CLASS*, model runs were conducted for each unique combination of attributes, and results allocated to the grid cells in which these combinations occurred. In *CBM-CFS3, Can-IBIS*, *InTEC* and *TRIPLEX*, a model run was conducted for each grid cell. Some model-specific protocols follow.

3.2.1. CBM-CFS3

The application of this model to the Chibougamau study area is described in detail in Bernier et al. (2010). Briefly, initial dead organic matter (DOM) and soil C stocks at the start of the study period in 1928 were estimated using a model spin-up procedure (Kurz et al., 2009). The AGC in 1928 was calculated using the inventory-based merchantable volume through the model's built-in volume to biomass conversion algorithm. Softwood and hardwood volumes were calculated separately for each polygon and converted to biomass C according to stand age estimated in 1928. Annual NPP increments from 1928 onwards were calculated from growth curves for each forest inventory analysis unit, i.e. black spruce, jack pine, balsam fir and trembling aspen, until a stand-replacing disturbance such as a clearcut occurred. After the stand-replacing disturbance, the stand age was reset to zero and the same growth curves were used to simulate NPP during forest regrowth, unless the stand management history indicated it had been planted in which case new growth curves were used. The value of R_h was calculated as the sum of DOM pool decomposition losses, computed as functions of a temperature modifier (Kurz et al., 2009). Net ecosystem productivity (NEP) was calculated as net primary productivity (NPP) minus heterotrophic respiration (R_h).

3.3. Process models

Ecosys was seeded with black spruce and/or trembling aspen with a moss understory in the model year 1808, run to 1928 under repeated sequences of weather data recorded at the EOBS flux tower, and then run to 2008 under the historical weather data. Clearcuts and plantings were modeled later in the 19th century so that stand ages modeled in 1928 for each grid cell were the same as those estimated from the 1928 aerial photos. Prescribed thinning was applied to simulate the background mortality rate generally observed during forest regrowth. Profiles of the different soil types were represented in *ecosys* by 6 to 8 layers to depths of 0.6–1.0 m as indicated in SLC 3.1.

Can-IBIS was initialized through a historical spin-up to 1928 conducted to stabilize ecosystem C pools. At this time, the biomass densities on every grid cell were adjusted to agree with AGC inferred from the 1928 aerial photos. *CN-CLASS* was initialized with the 1928 AGC provided for each grid cell by *CBM-CFS3*. This initial AGC was used to initialize biomasses of wood, heartwood, coarse root and fine root as 80%, 60%, 20% and 10% of AGC, respectively. The profile for each soil type in *CN-CLASS* was divided into three layers with thicknesses of 10 cm, 25 cm and 375 cm. In *InTEC*, C pools of biomass and soil were initialized assuming that CO_2 and N exchanges between the terrestrial ecosystems and the atmosphere were in equilibrium for those stands at equilibrium age under the mean conditions of climate, CO_2 concentration and N deposition in the pre-industrialization period (Wang et al., 2007). In *TRIPLEX*, initial 1928 values of tree density, tree height and diameter at breast height (DBH) were derived from AGC inferred from the 1928 aerial photos These models were then run from 1928 to either 2008 (*CN-CLASS* and *TRIPLEX*) or 2005 (*InTEC* and *Can-IBIS*) under the historical weather data.

3.4. Model tests and meta-analysis

The performances of two models operating on hourly time steps (*ecosys* and *CN-CLASS*) were compared by regressing mean CO_2 fluxes modeled for the grid cells within the EOBS tower fetch area with those measured by EC (i.e. excluding gap-filled values). The comparison was done for the coldest year 2004 (MAT = −0.4 °C) and the warmest year 2006 (MAT = +2.3 °C) of the 2004 to 2008 measurement period.

Model performance was considered to improve as intercepts from these regressions approached zero, and as slopes and coefficients of determination approached one. Further details of this comparison are given in Section 4.1. Simulation results from *Can-IBIS*, *InTEC* and *TRIPLEX* were available only for annual time steps, and were therefore compared against annually aggregated CO_2 flux measurements and annually aggregated results from the two hourly process models.

The capacity of the process models to reproduce the effect of seasonal variability in weather on annual NEP was tested by comparing the interannual variability of NEP simulated by each model to that derived from EOBS CO_2 flux measurements from 2004 to 2008. The spatial and temporal scales of the analysis were then extended to the entire Chibougamau study area and the decadal timescale by comparing measured changes in above-ground carbon (AGC) between 1928 and 1998 obtained from forest inventories, with the changes in AGC simulated by *CBM-CFS3* and all the process models, as affected by weather and disturbance.

The cross-model robustness of NEP and NPP responses to seasonal variability in weather were examined by relating annual variability in NEP and NPP to seasonal air temperature (T_a) and precipitation for all models on all grid cells. Stand age and forest disturbance effects on productivity during this period were removed by expressing annual NEP and NPP as deviations from their respective 7-year moving-averages during the period 1965–2005 when only modest disturbances were reported (Fig. 2). Correlations between these deviations and either seasonal T_a or precipitation were taken to indicate a modeled effect of these seasonal variables on annual NEP or NPP. Any effect that was significant and consistent across the diverse process models in this study was taken be robust. Only results pertaining to T_a are presented below as our tests revealed no significant correlation between seasonal precipitation and either NEP or NPP. Key algorithms by which model results were produced are given in the text with reference to Supplementary Material Table S1.

4. Results

4.1. Evaluating model performance

As mentioned earlier, among process models, only *ecosys* and *CN-CLASS* were run at hourly time steps for the coldest (2004) and warmest (2006) years of the measurement period. Differences in seasonal temperatures caused daily NEP to follow different time courses in 2004 and 2006 (Figs. 3 and 4). Earlier spring warming caused onset of net C uptake to occur on April 15 (DOY 105) in 2006 as compared to May 7 (DOY 128) in 2004 (Figs. 3b,c and 4b,c). The onset of net C uptake was quite rapid in both years, suggesting

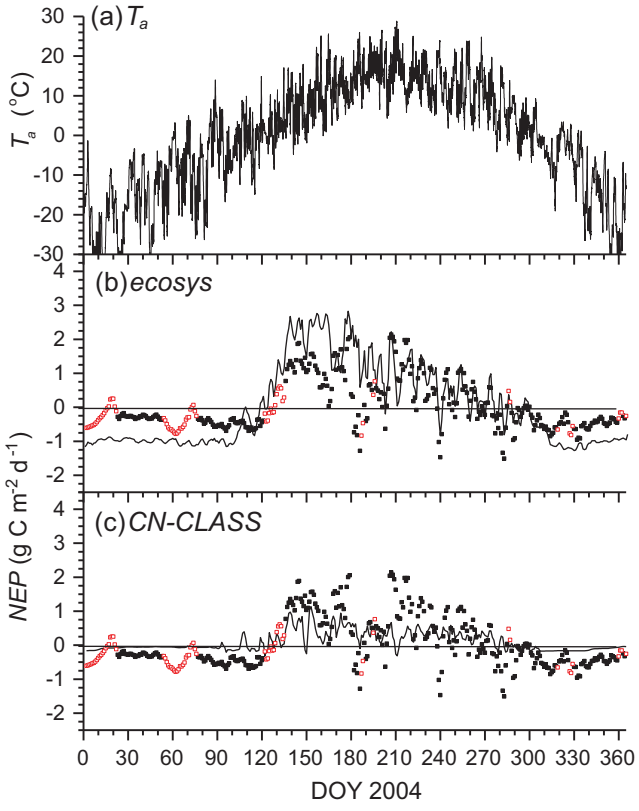

Fig. 3. (a) Hourly air temperature (a) and 3-day average of net ecosystem productivity (NEP) calculated from CO_2 fluxes measured by eddy covariance (closed symbols) or gap-filled from eddy covariance measurements (open symbols) and modeled (lines) by *ecosys* (b) and *CN-CLASS* (c) in flux tower fetch area during the coldest year, 2004.

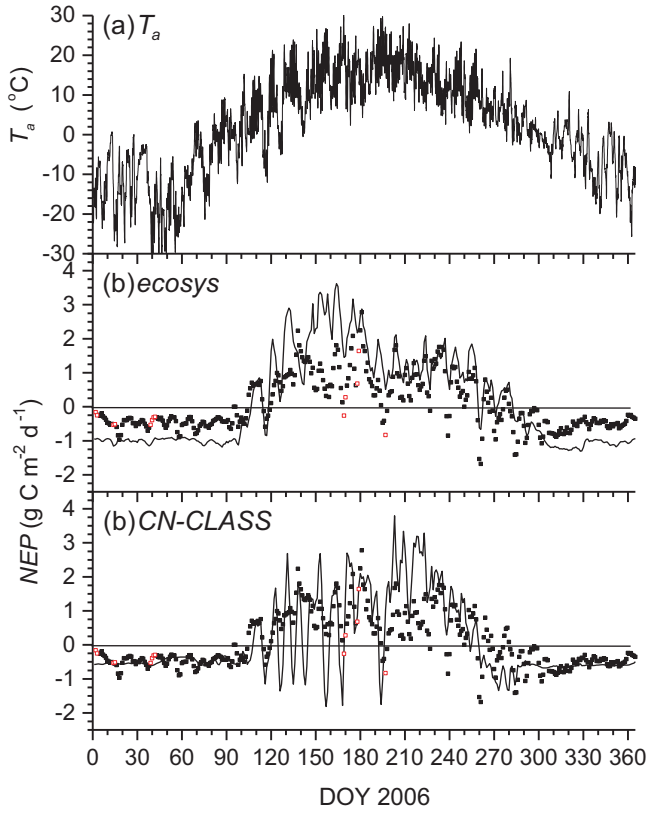

Fig. 4. (a) Hourly air temperature (a) and 3-day average of net ecosystem productivity (NEP) calculated from CO_2 fluxes measured by eddy covariance (closed symbols) or gap-filled from eddy covariance measurements (open symbols) and modeled (lines) by *ecosys* (b) and *CN-CLASS* (c) in flux tower fetch area during the warmest year, 2006.

activation of CO_2 fixation by a thermal signal in spring. The timing of this thermal signal was simulated with some accuracy by both process models, allowing the earlier onset of net C uptake to be simulated in 2006 than 2004. Given the rapid increase in CO_2 fixation following activation, accurate timing of this signal is important to accurately simulate NEP in boreal conifer forest ecosystems.

Net C uptake attained maximum values from late May to late June in both years (Figs. 3 and 4). During this period, *ecosys* overestimated net C uptake, consistent with its bias toward larger CO_2 fluxes detected in the regressions (Table 2), while *CN-CLASS* underestimated net C uptake. Net C uptake generally declined after late June in both years, particularly when T_a exceeded 25 °C, suggesting adverse effects of higher T_a on *NEP* during summer (Figs. 3 and 4). Higher T_c and D in *ecosys* forced lower ψ_c (A.1.3 in Table S1), g_l (A.2.1 in Table S1) and hence sharp declines in mid-afternoon CO_2 influxes (A.1.3) when $T_a > 25$ °C. This phenomenon was also apparent in the measured EC fluxes. Higher T_a caused much sharper declines of CO_2 influxes in *CN-CLASS* than were apparent in measured fluxes (Figs. 3c and 4c). These declines were attributed to the small D_0 value in *CN-CLASS* (A.2.1 in Table S1) that caused g_l, and hence CO_2 influxes, to decline sharply under rising D caused by warming (Arain et al., 2002). These declines in mid-afternoon CO_2 influxes caused the sharp declines in simulated net daily C uptake with warming in 2004 and 2006 (Figs. 3 and 4).

Overall, *ecosys* reproduced the variation in measured CO_2 fluxes with better accuracy under the range of weather conditions recorded from 2004 through 2008, as shown by the nearly unitary slopes of regressions of modeled versus measured hourly CO_2 fluxes (Table 2). The intercepts were slightly positive, indicating a modeling bias toward overestimation of fluxes. The corresponding

Table 2
Intercepts (a), slopes (b), coefficients of determination (R^2), root mean square of differences (RMSD) from regressions of hourly CO_2 fluxes by two process models vs. hourly-averaged CO_2 fluxes measured by EC from 2004 to 2008 in the fetch area of the EOBS flux tower.

Model	Year	MAT (°C)	a[a] (μmol m^{-2} s^{-1})	b	R^2	RMSD (μmol mm^{-2} s^{-1})	n
ecosys	2004	−0.3	0.16	0.93	0.74	1.65	5310
	2005	1.5	0.27	0.99	0.76	1.54	6531
	2006	2.3	0.20	1.02	0.76	1.47	6367
	2007	0.8	0.27	1.11	0.76	1.35	6367
	2008	1.2	0.20	1.04	0.80	1.40	6309
CN-CLASS	2004	−0.3	−0.11	0.83	0.63	1.96	5310
	2005	1.5	−0.06	0.60	0.36	2.54	6531
	2006	2.3	0.10	0.91	0.61	1.89	6367
	2007	0.8	0.11	0.83	0.51	1.95	6367
	2008	1.2	0.42	1.04	0.64	1.87	6309

[a] a, b and R^2 from regressions of modeled on measured fluxes, RSMD from regressions of measured on modeled fluxes.

regressions from *CN-CLASS* results gave intercepts closer to zero but slopes less than one in all years except 2008, indicating a modeling bias toward underestimation of variation in fluxes. For both models, root mean squares of differences between modeled and measured fluxes were less than, or similar to, a root mean square for error of 1.9 μmol m^{-2} s^{-1} estimated for CO_2 flux measurements at EOBS (Richardson et al., 2006). Some of the variation in measured CO_2 fluxes unexplained by the models could therefore be reasonably attributed to measurement uncertainty.

At the annual time step, measured NEP rose slightly with warming in 2006 vs. 2004 (MAT +2.3 °C vs. −0.4 °C), and then declined with subsequent cooling in 2007 and 2008 (MAT 0.8 °C and 1.2 °C) (Fig. 5). The simulated NEP from all five process models tested also rose from 2004 to 2006, although initial negative NEP from some of these models was not consistent with the small but positive NEP derived from gap-filled CO_2 flux measurements. Annual simulated NEP by *ecosys* rose slightly more with warming from 2004 to 2006 than did that from measurement, while annual NEP from *CN-CLASS* was below that from observation in 2004, but rose sharply with warming in 2006, as shown in Figs. 3 and 4. Annual values of NEP averaged across all process models were generally close to measured values (Fig. 5). The two more detailed models, *ecosys* and *CN-CLASS* did not simulate annual NEP more accurately than other models, but were better suited to more detailed and hence better-constrained tests (Figs. 3 and 4) that allowed causes of disagreement between simulated and measured fluxes to be investigated.

Differences in AGC between inventories in 1928 and 1988 provide a measure of process model performance at decadal and landscape scales (Fig. 6). The landscape-averaged increase in AGC between the 1928 and 1998 inventories at Chibougamau was 13.67 Mg C ha^{-1} and the corresponding AGC increase modeled by *CBM-CFS3* was 11.61 Mg C ha^{-1} (Bernier et al., 2010). By comparison, landscape-averaged AGC increases in the process models were 17.11 Mg C ha^{-1} (*ecosys*), 7.28 Mg C ha^{-1}(*Can-IBIS*), 26.22 Mg C ha^{-1} (*CN-CLASS*), 11.02 Mg C ha^{-1} (*InTEC*), and 10.73 Mg C ha^{-1} (*TRIPLEX*). Differences among models in cumulative net biome productivity (NBP) resulted in part from differences in long-term rates of C accrual, and in part from differences in responses to the disturbances in the mid-1960s (Fig. 7). Although a common set of disturbance coefficients was used to model harvesting effects on AGC and BGC, considerable divergence for these effects nonetheless occurred among models (Fig. 7a and b). This divergence was attributed to the application of these coefficients to model-specific variables for different C stocks, indicating an area requiring improvement in process models.

4.2. Defining climatic drivers of CO_2 flux variability

Deviations in modeled annual NEP from its 7-year running average were positively correlated with spring T_{amax} in results from only *ecosys* and *InTEC* (Fig. 8). There was no comparable significant correlation in *CN-CLASS* results (Fig. 8), although earlier spring warming hastened simulated net C uptake (Figs. 3 and 4) (e.g. Grant et al., 2009a,b). Deviations in modeled annual NEP from its 7-year running average were negatively correlated with summer T_{amax} only in results from *CN-CLASS* (R^2 = 0.4, Fig. 9) consistent with its large decline of daily NEP under higher T_a (Fig. 4).

Deviations in annual NPP were positively correlated with spring T_{amax} in both the hourly process models *ecosys* and *CN-CLASS* (Fig. 10). Significant positive correlations were also found in two of the other three process models, *InTEC* and TRIPLEX, but not in *Can-IBIS* (Fig. 10). By contrast, deviations in annual NPP were negatively correlated to summer T_{amax} only in *CN-CLASS* (R^2 = 0.2) (Fig. 11). No interannual variability in NPP was modeled by *CBM-CFS3* as its modeling process does not allow for NPP to respond to climatic variability.

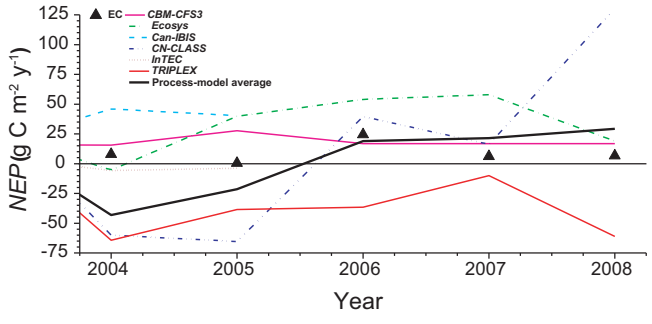

Fig. 5. Modeled and eddy covariance-derived annual values of net ecosystem productivity (NEP) in flux tower fetch area during 2004–2008.

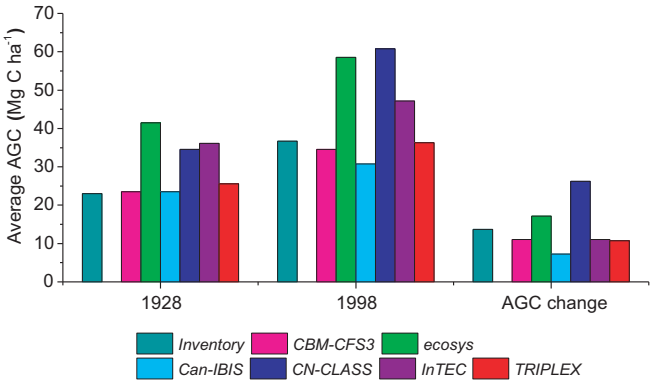

Fig. 6. Above-ground carbon in biomass (AGC), and 1928–1998 change in AGC from inventory and as estimated from various models.

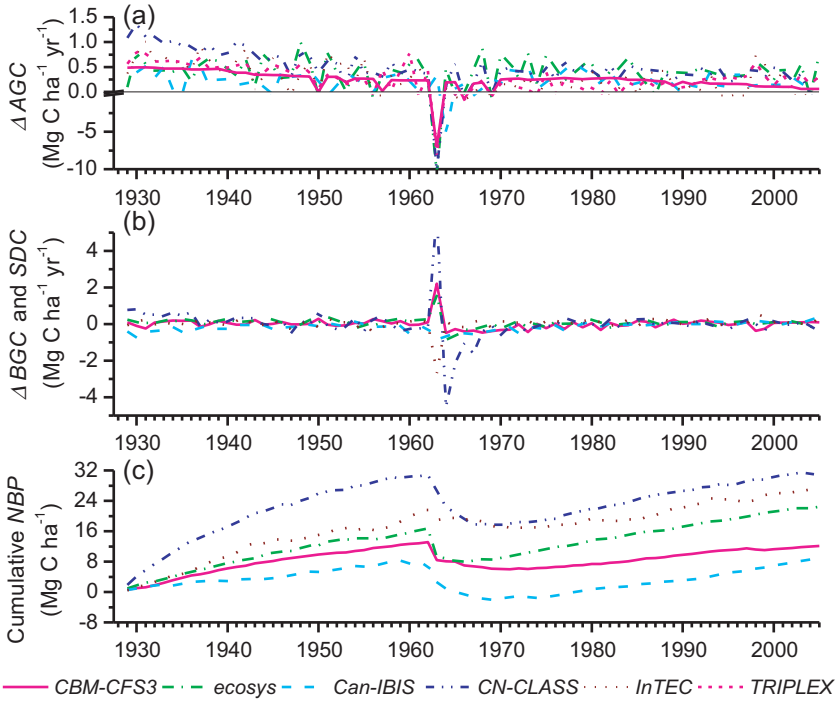

Fig. 7. Annual changes in average above-ground living biomass C (AGC), below-ground C (BGC) and surface dead organic C (SDC), and cumulative net biome productivity (NBP) modeled in all forested grid cells in the study area during the 1928–2005 period.

4.3. Incorporating climate in inventory models

The positive relationship between spring T_{amax} and annual NPP found to be significant in *ecosys*, *CN-CLASS*, *InTEC* and *TRIPLEX* (Fig. 10) was considered consistent enough to be summarized for use in inventory models, expressed as:

$$\mathrm{NPP}'_i = \mathrm{NPP}_i + 9.5(T_{amax} - 16.5) \quad (1)$$

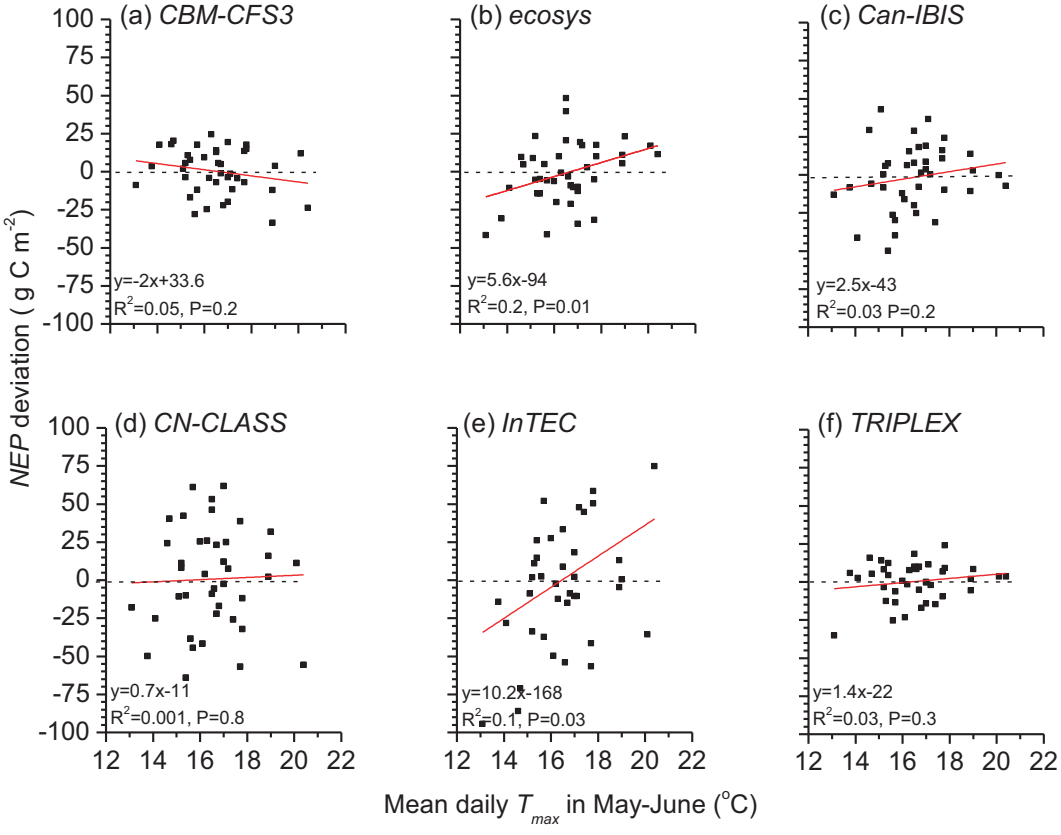

Fig. 8. Regressions of modeled yearly annual net ecosystem productivity (NEP) deviations to mean daily maximum temperature (T_{max}) in spring during 1965–2005.

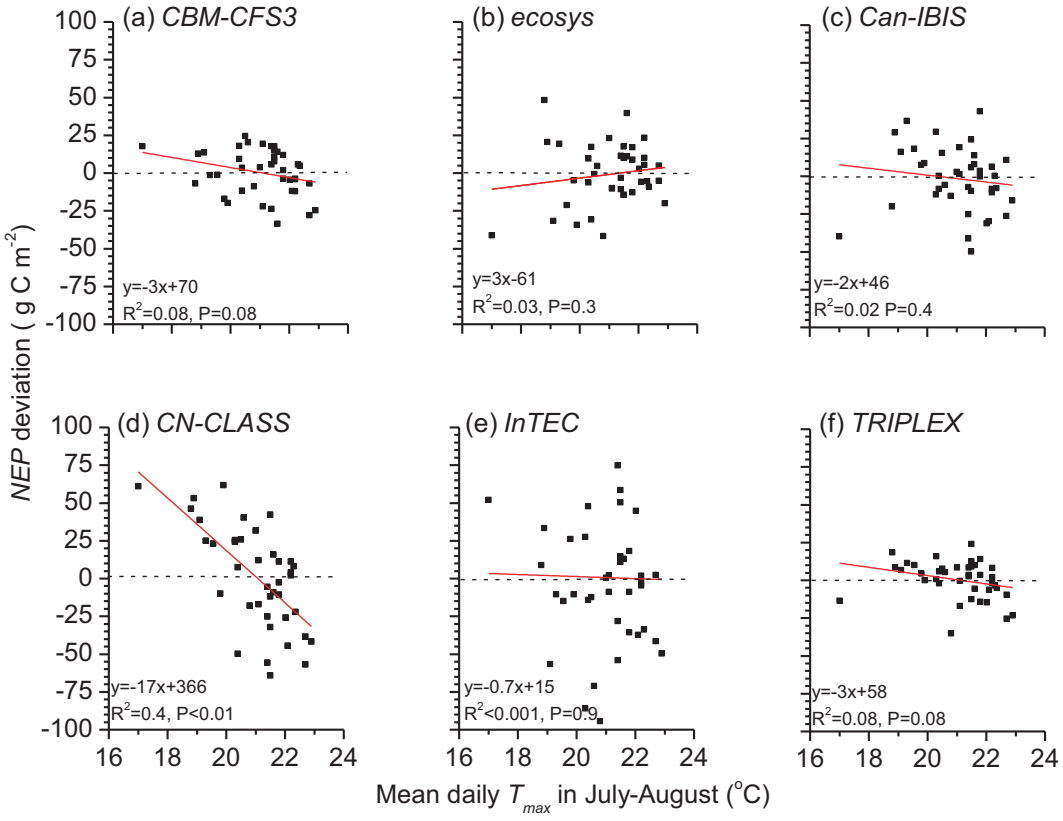

Fig. 9. Regressions of modeled annual net ecosystem productivity (NEP) deviations to mean daily maximum temperature (T_{max}) in summer during 1965–2005.

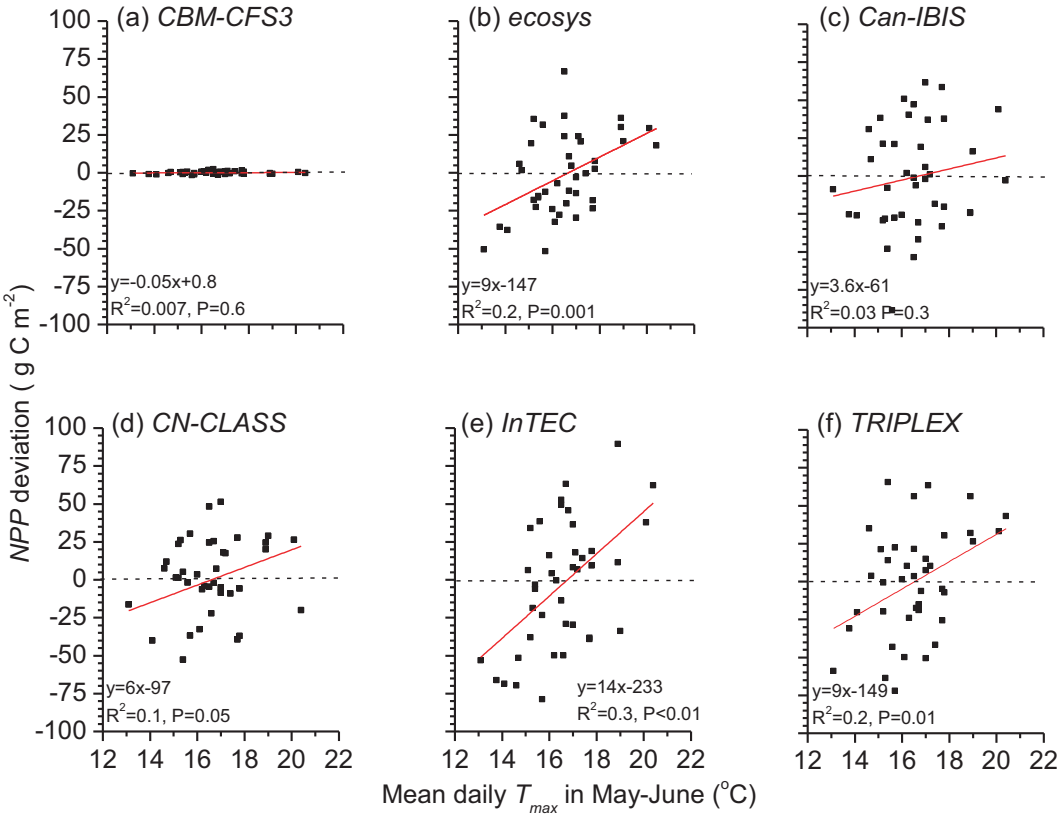

Fig. 10. Regressions of modeled annual net primary productivity (NPP) deviations on mean daily maximum temperature (T_{max}) in spring during 1965–2004.

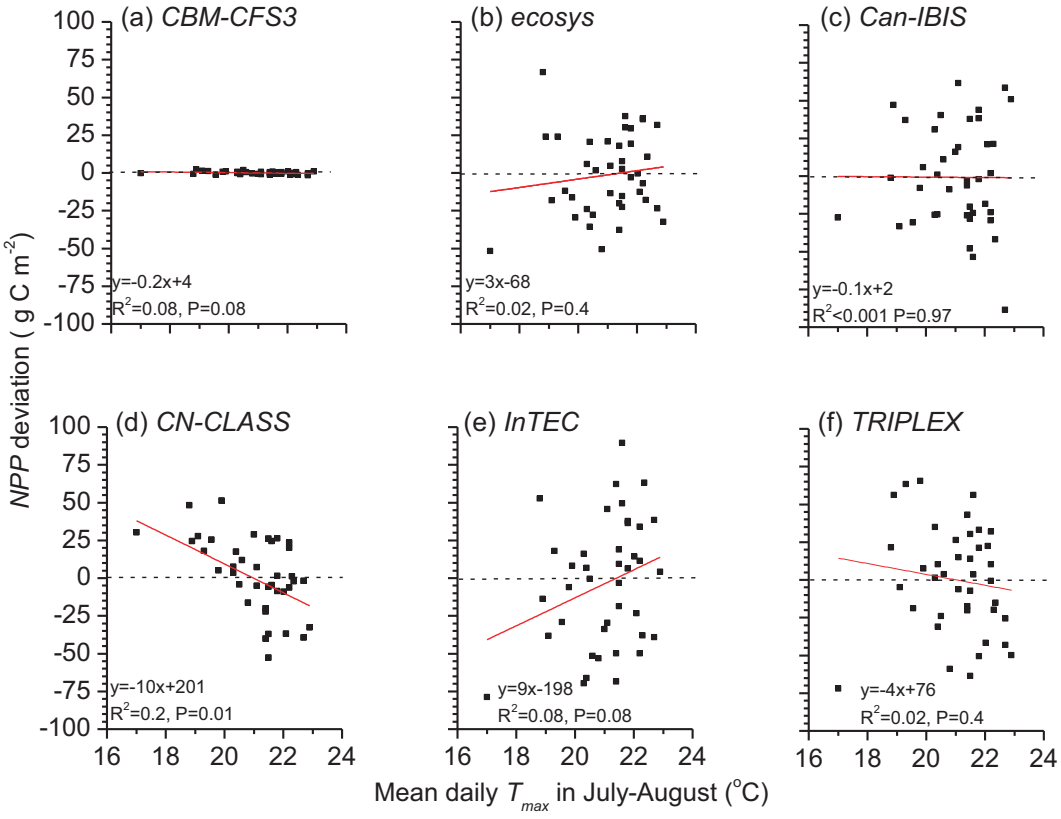

Fig. 11. Regressions of modeled annual net primary productivity (NPP) deviations on mean daily maximum temperature (T_{max}) in summer during 1965–2004.

where NPP'_i is the temperature-adjusted annual NPP ($g\,C\,m^{-2}\,y^{-1}$), NPP_i is the unadjusted NPP currently estimated by *CBM-CFS3* ($g\,C\,m^{-2}\,y^{-1}$), 9.5 is the average slope of the four significant regressions in Fig. 10 ($g\,C\,m^{-2}\,y^{-1}\,°C^{-1}$), T_{amax} is the average daily maximum T_a in May and June in a given year (°C), and 16.5 is the long-term average T_{amax} in May and June in the Chibougamau landscape.

5. Discussion

5.1. Relationship between NPP and T_a in boreal climates

The summary relationship presented above was derived from a meta-analysis of results from four process models in which temperature effects on GPP and R_a were developed independently. Coherence of results among the majority of these models indicates that this relationship is robust. The NPP slope parameter of $9.5\,g\,C\,m^{-2}\,y^{-1}\,°C^{-1}$ is similar to values of 15.6 and $5.0\,g\,C\,m^{-2}\,y^{-1}\,°C^{-1}$ derived for NPP relationships with T_a in April and May by Tang et al. (2010) for a range of forest types, including boreal conifers, in New England where NPP was slightly larger than that in our study. This similarity suggests a broader applicability of these results. The parameter of $9.5\,g\,C\,m^{-2}\,y^{-1}\,°C^{-1}$ derived in this study would also account for the gain of $12\,g\,C\,m^{-2}$ in net CO_2 uptake recorded over a boreal coniferous forest by Delpierre et al. (2009) with an increase in spring T_a of 1–2 °C during the anomalously warm spring of 2007 in Europe.

The relationship presented in this boreal black spruce landscape is also consistent with findings from tree ring studies in which annual growth of black spruce was positively correlated with monthly average T_a during May and June, but not during July and August, in the continental boreal climate of western Labrador (Nishimura and Laroque, 2011). However, this relationship may be limited to continental boreal climates because these same studies indicated that annual growth of black spruce was better correlated with monthly average T_a during July than in May or June in maritime boreal climates in eastern Labrador, where summer T_a was lower (Nishimura and Laroque, 2011).

5.2. Relationship between NPP and T_a in boreal vs. temperate climates

The relationship of annual NPP with spring T_{amax} in this study differs from the results of an earlier study with the same modeling protocol in a western coastal temperate Douglas-fir landscape where annual NPP was found to be most strongly related to summer T_{amax} (Wang et al., 2011). The NPP slope parameter for the temperate landscape was $-57.1\,g\,C\,m^{-2}\,y^{-1}\,°C^{-1}$ as compared to $+9.5\,g\,C\,m^{-2}\,y^{-1}\,°C^{-1}$ in this study, indicating large differences in the sensitivity of NPP to T_a between the two landscapes. Mean annual temperature is 0 °C vs. 8.4 °C for the boreal vs. temperate landscape, indicating greater temperature constraints to NPP in the former, particularly in spring.

The difference in the response of NPP to T_a between our two modeling studies is consistent with findings from field observations. The negative relationship between NPP and summer T_{amax} modeled for a coastal temperate Douglas-fir (Wang et al., 2011) has been found in drier boreal and temperate climate zones in western North America, in Douglas-fir (Falk et al., 2008), black spruce (Dang and Lieffers, 1989) and other conifers (Barber et al., 2000; Wilmking et al., 2004). Hofgaard et al. (1999) also found that the dominant controls on growth of black spruce change from a positive effect of spring T_a in colder climates such as that at Chibougamau where black spruce is dominant, to a negative effect of summer T_a in warmer climates near the southern limit of black spruce.

5.3. Relationship between NEP and T_a

The lack of relationship between NEP and either spring or summer T_a contrasts with the robust relationship established between NPP and spring T_{amax}. NEP is a net flux, the difference between the photosynthetic carbon uptake and R_e, the sum of R_a and R_h. R_a is the sum of maintenance and growth respiration, both of which increase with greater growth and T_a. However, R_h is driven by soil temperature and by litterfall, and so may not be consistently related to current T_a. Simulation results (Figs. S1 and S2 in the Supplementary Material) did suggest increased R_h with increased spring T_a, although the relationship was not as robust as that with NPP. We therefore expected to find at best a weak relationship between NEP and spring T_a.

5.4. Application of the relationship between NPP and T_a in inventory models

Although the correlation coefficients of spring T_{amax} with NPP among the process models are low (Fig. 10), they are comparable to those of monthly T_a with radial growth indices in the tree ring studies of Hofgaard et al. (1999) and Nishimura and Laroque (2011), indicating that interannual variation in monthly spring T_a explains only a fraction of the variation in NPP. The incorporation of this relationship into models used to calculate national forest inventories in continental boreal ecozones could nonetheless account for much of the interannual variation in the growth seen in these inventories. Given the range in spring T_{amax} of $\pm 3.5\,^{\circ}C$ about the mean in this study (Fig. 10), this relationship would cause a range in NPP of $\pm 33\,g\,C\,m^{-2}\,y^{-1}$ to be calculated about the current mean of $275\,g\,C\,m^{-2}\,y^{-1}$ estimated for the Chibougamau region. This range is similar to the interannual variation of 0.15–0.20 in standardized radial growth indices of black spruce measured by Hofgaard et al. (1999) in Quebec, and by Nishimura and Laroque (2011) in Labrador, significant fractions of which were associated with spring T_a in continental boreal climates.

Overall, the relationships between NPP and T_a developed in this study and in Wang et al. (2011) provide a process-based methodology to incorporate climate sensitivity into inventory-based models such as CBM-CFS3. These relationships would help to capture effects of climate variability on C inventories for two major Canadian forest ecozones, i.e. eastern boreal black spruce and western temperate Douglas-fir ecozone. These two studies also provide a demonstration of concept for the derivation of simple climate modifier functions from the meta-analysis of results from process-based models for application to C inventory models.

6. Conclusions

The model results from which the relationship between spring T_{amax} and annual NPP was derived were generated from almost 4000 grid cells representing a range of soil and plant types found in many Canadian boreal landscapes, and should therefore be scalable to other regions with a humid continental boreal climate dominated by black spruce. Collectively, such regions comprise one of the largest climatic zones in the 450 Mha North American boreal forests (Viereck and Johnston, 1990). Because of the extent of the boreal forest, application of this small climate modifier to the evaluation of NPP may be of consequence when estimating the sensitivity of boreal coniferous C stocks to variability and possibly trends in climate for national forest inventories.

This study also highlights areas in process models that need improvements. Of particular concern is the divergence in model responses to transitory processes associated with disturbances. This divergence may indicate a lack of appropriate experimental data on which models can be parameterized or validated. More fundamentally, the divergence may result from a lack of consistent knowledge or broader inferences with respect to the magnitude and timing of individual C fluxes in the few critical years that follow disturbances. This gap must be addressed if we want to predict how forest C will react to a changing climate, particularly in boreal ecosystems where natural disturbances are a dominant process over large areas.

Acknowledgements

These results are part of the historical carbon modeling project of the Fluxnet Canada Research Network/Canadian Carbon Program whose financial support was provided by the Natural Science and Engineering Research Council, the Canadian Foundation for Climate and Atmospheric Science, Natural Resources Canada and BIOCAP. *Ecosys* model runs were done on the AICT Linux Cluster at the University of Alberta and the WestGrid Glacier cluster at the University of British Columbia. CN-CLASS model runs were made at the SHARCNET at the McMaster University. We want to thank the two anonymous reviewers whose constructive comments have helped us improve our text.

Appendix A. Supplementary data

Supplementary data associated with this article can be found, in the online version, at http://dx.doi.org/10.1016/j.ecolmodel.2013.03.016.

References

Amiro, B.D., Stocks, B.J., Alexander, M.E., Flannigan, M.D., Wotton, B.M., 2001. Fire, climate change, carbon and fuel management in the Canadian boreal forest. International Journal of Wildland Fire 10, 405–413.

Arain, M.A., Black, T.A., Barr, A.G., Jarvis, P.G., Massheder, J.M., Verseghy, D.L., Nesic, Z., 2002. Effects of seasonal and interannual climate variability on net ecosystem productivity of boreal deciduous and conifer forests. Canadian Journal of Forest Research 32 (5), 878–891.

Arain, M.A., Yuan, F., Black, T.A., 2006. Soil–plant nitrogen cycling modulated carbon exchanges in a western temperate conifer forest in Canada. Agricultural and Forest Meteorology 140, 171–192.

Banfield, G.E., Bhatti, J.S., Jiang, H., Apps, M.J., 2002. Variability in regional scale estimates of carbon stocks in boreal forest ecosystems: results from west-central Alberta. Forest Ecology and Management 169 (1–2), 15–27.

Barber, V.A., Juday, G.P., Finney, B.P., 2000. Reduced growth of Alaska white spruce in the twentieth century from temperature-induced drought stress. Nature 405, 668–673.

Barr, A.G., Black, T.A., Hogg, E.H., Kljun, N., Morgenstern, K., Nesic, Z., 2004. Interannual variability in the leaf area index of a boreal aspen–hazelnut forest in relation to net ecosystem production. Agricultural and Forest Meteorology 126 (3–4), 237–255.

Bergeron, O., Margolis, H.A., Black, T.A., Coursolle, C., Dunn, A.L., Barr, A.G., Wofsy, S.C., 2007. Comparison of carbon dioxide fluxes over three boreal black spruce forests in Canada. Global Change Biology 13, 89–107.

Bernier, P.Y., Guindon, L., Kurz, W.A., Stinson, G., 2010. Reconstructing and modelling 71 years of forest growth in a Canadian boreal landscape: a test of the CBM-CFS3 carbon accounting model. Canadian Journal of Forest Research 40 (1), 109–118.

Bossel, H., 1996. TREEDYN3 forest simulation model. Ecological Modelling 90, 187–227.

Brooks, J.R., Flanagan, L.B., Ehleringer, J.R., 1998. Responses of boreal conifers to climate fluctuations: indications from tree-ring widths and carbon isotope analyses. Canadian Journal of Forest Research 28, 524–533.

Canadian Forest Service, 2009. The State of Canada's Forests 2009. Natural Resources Canada, Ottawa.

CanSIS, 2006. Soil Survey Data for British Columbia: Southern Vancouver Island. Agriculture and Agri-Food Canada http://www.sis.agr.gc.ca/cansis/nsdb/detailed/bc/southvani.zip

Chen, W., Chen, J., Cihlar, J., 2000. An integrated terrestrial ecosystem carbon-budget model based on changes in disturbance, climate, and atmospheric chemistry. Ecological Modelling 135, 55–79.

Chen, J.M., Ju, W., Cihlar, J., Price, D., Liu, J., Chen, W., Pan, J., Black, A., Barr, A., 2003. Spatial distribution of carbon sources and sinks in Canada's forests. Tellus, Series B: Chemical and Physical Meteorology 55, 622–641.

Chertov, O., Bhatti, J.S., Komarov, A., Mikhailov, A., Bykhovets, S., 2009. Influence of climate change, fire and harvest on the carbon dynamics of black spruce in central Canada. Forest Ecology and Management 257, 941–950.

Coursolle, C., Margolis, H.A., Barr, A.G., Black, T.A., Amiro, B.D., McCaughey, J.H., Flanagan, L.B., Lafleur, P.M., Roulet, N.T., Bourque, C.P.-A., Arain, M.A., Wofsy, S.C., Dunn, A., Morgenstern, K., Orchansky, A.L., Bernier, P.Y., Chen, J.M., Kidston, J., Saigusa, N., Hedstrom, N., 2006. Late-summer carbon fluxes from Canadian forests and peatlands along an east–west continental transect. Canadian Journal of Forest Research 36 (3), 783–800.

D'Arrigo, R., Jacoby, G.C., Fung, I.Y., 1987. Boreal forests and atmosphere–biosphere exchange of carbon dioxide. Nature 329, 321–323.

Dang, Q.L., Lieffers, V.J., 1989. Climate and annual ring growth of black spruce in some Alberta peatlands. Canadian Journal of Botany 67, 1885–1889.

Delpierre, N., Soudani, K., François, C., Köstner, B., Pontailler, J.Y., Nikinmaa, E., Misson, L., Aubinet, M., Bernhofer, C., Granier, A., Grűnwald, T., Heinesch, B., Longdoz, B., Ourcival, J.M., Rambal, S., Vesala, T., Dufrêne, E., 2009. Exceptional carbon uptake in European forests during the warm spring of 2007: a data–model analysis. Global Change Biology 15, 1455–1474.

Falk, M., Wharton, S., Schroeder, M., Ustin, S., Paw, U.K.T., 2008. Flux partitioning in an old-growth forest: seasonal and interannual dynamics. Tree Physiology 28, 509–520.

Goetz, S.J., Bunn, A.G., Fiske, G.J., Houghton, R.A., 2005. Satellite-observed photosynthetic trends across boreal North America associated with climate and fire disturbance. Proceedings of the National Academy of Science 102, 13521–13525.

Grant, R.F., Arain, A., Arora, V., Barr, A., Black, T.A., Chen, J., Wang, S., Yuan, F., Zhang, Y., 2005. Intercomparison of techniques to model high temperature effects on CO_2 and energy exchange in temperate and boreal coniferous forests. Ecological Modelling 188 (2–4), 217–252.

Grant, R.F., Barr, A.G., Black, T.A., Gaumont-Guay, D., Iwashita, H., Kidson, J., et al., 2007. Net ecosystem productivity of boreal jack pine stands regenerating from clearcutting under current and future climates. Global Change Biology 13 (7), 1423–1440.

Grant, R.F., Barr, A.G., Black, T.A., Margolis, H.A., Dunn, A.L., Metsaranta, J., Wang, S., 2009a. Interannual variation in net ecosystem productivity of Canadian forests as affected by regional weather patterns – a Fluxnet-Canada synthesis. Agricultural and Forest Meteorology 149, 2022–2039.

Grant, R.F., Margolis, H.A., Barr, A.G., Black, T.A., Dunn, A.L., Bernier, P.Y., Bergeron, O., 2009b. Changes in net ecosystem productivity of boreal black spruce stands in response to changes in temperature at diurnal and seasonal timescales. Tree Physiology 29 (1), 1–17.

Griffis, T.J., Black, T.A., Morgenstern, K., Barr, A.G., Nesic, Z., Drewitt, G.B., Gaumont-Guay, D., McCaughey, J.H., 2003. Ecophysiological controls on the carbon balances of three southern boreal forests. Agricultural and Forest Meteorology 117, 53–71.

Hofgaard, A., Tardif, J., Bergeron, Y., 1999. Dendroclimatic response of Picea mariana and Pinus banksiana along a latitudinal gradient in the eastern Canadian boreal forest. Canadian Journal of Forest Research 29 (9), 1333–1346.

Kang, S., Kimball, J., Running, S., 2006. Simulating effects of fire disturbance and climate change on boreal forest productivity and evapotranspiration. Science of the Total Environment 362, 85–102.

Kurz, W.A., Apps, M.J., 2006. Developing Canada's national forest carbon monitoring, accounting and reporting system to meet the reporting requirements of the Kyoto Protocol. Mitig. Adapt. Strategies Glob. Change 11 (1), 33–43.

Kurz, W.A., Dymond, C.C., White, T.M., Stinson, G., Shaw, C.H., Rampley, G.J., Smyth, C., Simpson, B.N., Neilson, E.T., Trofymow, J.A., Metsaranta, J., Apps, M.J., 2009. CBM-CFS3: a model of carbon-dynamics in forest and land-use change implementing IPCC standards. Ecological Modelling 220, 480–504.

Landsberg, J.J., Waring, R.H., 1997. A generalised model of forest productivity using simplified concepts of radiation-use efficiency, carbon balance and partitioning. Forest Ecology and Management 95, 209–228.

Liu, J.X., Peng, C.H., Dang, Q.L., Apps, M.J., Jiang, H., 2002. A component objective model strategy for reusing ecosystem models. Computers and Electronics in Agriculture 35, 17–33.

Liu, J., Price, D.T., Chen, J.M., 2005. Nitrogen controls on ecosystem carbon sequestration: Aa model implementation and application to Saskatchewan, Canada. Ecological Modelling 186 (2), 178–195.

Margolis, H.A., Flanagan, L.B., Amiro, B.D., 2006. The Fluxnet-Canada Research Network: influence of climate and disturbance on carbon cycling in forests and peatlands. Agricultural and Forest Meteorology 140, 1–5.

Morgenstern, K., Black, T.A., Humphreys, E.R., Griffis, T.J., Drewitt, G.B., Cai, T., Nesic, Z., Spittlehouse, D.L., Livingstone, N.J., 2004. Sensitivity and uncertainty in the carbon balance of a Pacific northwest Douglas fir forest during an El Niño/El Niña cycle. Agricultural and Forest Meteorology 123, 201–219.

Nishimura, P.H., Laroque, C.P., 2011. Observed continentality in radial growth–climate relationships in a twelve site network in western Labrador, Canada. Dendrochronologia 29, 17–23.

Parton, W.J., Scurlock, J.M., Ojima, D.S., Gilmanov, T.G., Scholes, R.J., Schimel, D.S., Kirchner, T., Menaut, J.-C., Seastedt, T., Garcia Moya, E., Kamnalrut, A., Kinyamario, J.I., 1993. Observations and modelling of biomass and soil organic matter dynamics for the grassland biome worldwide. Global Biogeochemical Cycles 7, 785–809.

Peng, C., Liu, J., Dang, Q., Apps, M.J., Jiang, H., 2002. TRIPLEX: a generic hybrid model for predicting forest growth and carbon and nitrogen dynamics. Ecological Modelling 153, 109–130.

Rapalee, G., Trumbore, S.E., Davidson, E.A., Harden, J.W., Veldhuis, H., 1998. Soil carbon stocks and their rate of accumulation and loss in a boreal forest landscape. Global Biogeochemical Cycle 12, 687–701.

Richardson, A.D., Hollinger, D.Y., Burba, G.G., Davis, K., Flanagan, L.B., et al., 2006. A multi-site analysis of random error in tower-based measurements of carbon and energy fluxes. Agricultural and Forest Meteorology 136, 1–18.

Savva, Y., Bergeron, Y., Denneler, B., Koubaa, A., Tremblay, F., 2008. Effect of interannual climate variations on radial growth of jack pine provenances in Petawawa, Ontario. Canadian Journal of Forest Research 38, 619–630.

Sun, J., Peng, C., McCaughey, H., Zhou, X., Thomas, V., Berninger, F., St-Onged, B., Hua, D., 2008. Simulating carbon exchange of Canadian boreal forests. II. Comparing the carbon budgets of a boreal mixedwood stand to a black spruce forest stand. Ecological Modelling 219, 276–286.

Tang, G., Beckage, B., Smith, B., Miller, P.A., 2010. Estimating potential forest NPP, biomass and their climatic sensitivity in New England using a dynamic ecosystem model. Ecosphere 1 (6), 1, http://dx.doi.org/10.1890/ES10-00087 (art 18).

Viereck, L.A., Johnston, W.F., 1990. *Picea mariana* (Mill.) B.S.P. In: Burns, R.M., Honkala, B.H. (Eds.), Silvics of North America. Vol. 1. Conifers, Agricultural Handbook 654. USDA Forest Service, pp. 227–237.

Wang, S., Chen, J., Ju, W., Feng, X., Chen, M., Chen, P., Yu, G., 2007. Carbon sinks and sources in China's forests during 1901–2001. Journal of Environmental Management 85, 524–537.

Wang, Z., Grant, R.F., Arain, M.A., Chen, B., Coops, N., Hember, R., Kurz, W.A., Price, D.T., Stinson, G., Trofymow, J.A. and Yeluripati, J., Model intercomparison to evaluate climate effect on interannual variation in net ecosystem productivity of a coastal temperate forest landscape. Ecological Modelling. 222 (17), 2011, 3236-3249.

Wilmking, M., Juday, G.P., Barber, V.A., Zald, H.J., 2004. Recent climate warming forces contrasting growth responses of white spruce at treeline in Alaska through temperature thresholds. Global Change Biology 10, 1724–1736.